Macromolecules

pubs.acs.org/Macromolecules Article

Effects of the Ionizable Monomer Fraction on the Swelling Behavior of Weak Polyelectrolyte Brushes

Shahryar Ramezani Bajgiran, Farshad Safi Samghabadi, Si Li, Jacinta C. Conrad,* and Amanda B. Marciel*

Cite This: *Macromolecules* 2023, 56, 9218–9228 Read Online

ACCESS | Metrics & More | Article Recommendations | Supporting Information

ABSTRACT: Through a combination of in situ ellipsometry and streaming zeta potential measurements, we investigated the swelling behavior of weak polybasic brushes as a function of pH and the fraction of ionizable monomers *f*. The fraction of the ionizable monomer (2-(dimethylamino)ethyl acrylate, DMAEA) was precisely tuned by mixing a neutral hydrophilic monomer (2-hydroxyethyl acrylate, HEA) from $f = 1.00$ to $f = 0.00$. All charge containing fractions show pH-responsive behavior. At acidic pH, the brushes are within the strongly charged osmotic brush regime, and the swelling ratio increases with increasing *f*, qualitatively agreeing with the scaling laws for polyelectrolyte brushes (PEBs). Moreover, as the fraction of DMAEA is increased, the transition pH (pH*) shifts to more basic values, indicating that ionization becomes more favorable with increasing *f*. In the intermediate pH range, all charge-containing fractions show hysteretic behavior, where the pH* values in the backward direction shift to more acidic values, and the extent of hysteresis increases with *f*. Streaming zeta potential measurements are in good agreement with the observed brush swelling behavior at the minimum and maximum pH ranges for all fractions. However, the isoelectric point (pI) values are consistently larger than the pH* values with no appreciable hysteresis present in the zeta potential measurement cycles. We propose the hydrophobic periphery mechanism as the source of hysteresis in the swelling experiments and hypothesize that the origin of the disparity between pI and pH* is the probing length scale differences between the two methods. These findings elucidate the effects of charge on the swelling behavior and charge state of PEBs, which can lead to tailored pH-responsive surfaces for many applications.

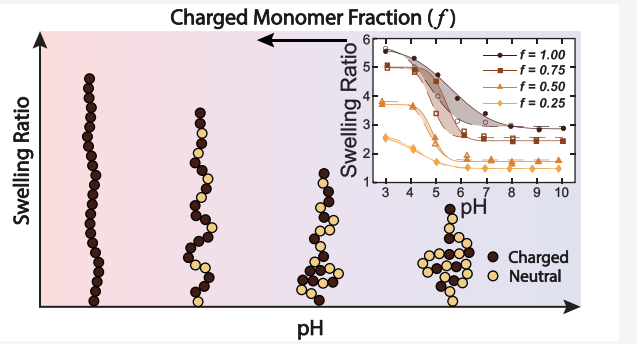

INTRODUCTION

Polymers end-tethered to planar and spherical surfaces are used to modify interfacial behavior of complex materials for applications requiring antifouling,[1−3] colloidal stabilization,[4] lubrication,[5,6] and separations.[7,8] The conformation of polymer chains at the interface is influenced by grafting density and chain length, where brush or mushroom-like conformations form at high and low grafting densities, respectively.[9] Monomer chemistry also affects the chain conformation. For example, strong polyelectrolyte brushes (PEBs) have more extended chain conformations than neutral brushes through balancing osmotic pressure and chain stretching.[10]

Weak PEBs are particularly interesting because the degree of ionization α is dependent on the ionic strength and pH of the solution. These dependencies generate two major challenges for predicting weak PEB behavior. First, weak (and strong) PEB behavior is incompletely described by the current theories. At low ionic strength and high dissociation ($\alpha \approx 1$), weak PEBs exhibit scaling relationships akin to those for strong PEBs in the osmotic brush (OB) regime, where brush height is independent of either grafting density σ or salt concentration C_s and height scales as $H \sim N\alpha^{1/2}$, where N is the number of repeat units in the brush chains.[10−12] By contrast, for weak PEBs with $\alpha \ll 1$ and salt concentrations below the crossover salt concentration C_s^* ($C_s \ll C_s^*$), height is theoretically predicted to scale as $H \sim N\sigma^{-1/3}([H^+] + C_s)^{1/3}$. Thus, increasing ionic strength or grafting density would result in an increase or decrease in brush height, respectively.[13] Whereas experiments have reproduced the predicted scaling exponents for N and C_s, a variety of power law values for σ have been reported, counter to theory.[14,15] At high salt concentrations ($C_s \geq C_s^*$), weak PEBs are once again predicted to behave similar to strong PEBs in the salted brush (SB) regime where brush height scales as $H \sim N\sigma^{1/3}C_s^{-1/3}\alpha^{2/3}$.

Received: May 15, 2023
Revised: October 18, 2023
Accepted: October 24, 2023
Published: November 10, 2023

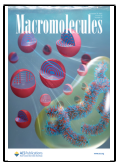

Experimental observations have generally agreed with the predicted nonmonotonic trends with increased salt concentration across the transition from the osmotic to salted brush regime.[14,15] Strong PEBs, however, also exhibit a nonmonotonic dependence on salt concentration, in disagreement with theory.[16] Differences between theory and experiments for both weak and strong PEBs speak to the need for experiments that systematically vary parameters, including chain length, density, and pH, to map out ranges of behavior for tests of theories.

Second, the pH-dependent behavior of weak PEBs is not fully understood despite extensive studies due to the complexity in ionization normal to the brush tether point. Ionization along weak PEB chains is nonuniform, and groups at the brush periphery dissociate with more ease.[13,17,18] This phenomenon has been attributed to the free energy minimization of the weak PEBs that inhibits ionization of monomers deeper in the brush, inhomogeneous volume fraction normal to the surface that slows down the uptake of water and ions into deeper denser regions of PEBs, and larger relative permittivity and accessibility of solution ions at the brush periphery.[13,17] In addition, the dissociation of groups on the periphery may lead to a double layer and create a boundary potential, thus further reducing ion transport inside the brush and preventing dissociation close to the surface.[17] Increasing C_s results in more uniform ionization as counterions from the salt can replace hydroxide and hydronium ions in the brush layer and promote more uniform charging of the acidic or basic moieties.[17,19] The complex dissociation behavior of weak PEBs makes it challenging to predict whether strong or weak PEB theory is applicable under a given experimental condition. Weak PEBs that include conditions where chains approach neutrality will enable more direct testing of the weak PEB theory.

Recent developments in surface-initiated polymerization techniques allow the synthesis of complex architectures that enable new tests of the open questions in the behavior of weak PEBs. Specifically, random copolymer PEBs, in which the monomers are distributed randomly along the brush chains, are readily synthesized by varying the fraction of ionizable monomers by mixing them with a neutral monomer. This approach is a straightforward strategy to achieve targeted brush properties without the need to change the charged monomer itself. Moreover, the neutral monomer can introduce another stimulus, resulting in multiresponsive brushes.[20−24] These previous experimental studies have found that charge effects can dominate chain conformation even at a low fraction of ionizable monomers and that weak PEBs with $f < 1$ act as weaker electrolytes than their homopolymeric counterparts. Although these studies have shown that varying the charge fraction imparts tunability over the brush architecture, they have not explored the full range of the ionizable monomer fraction or its effect on brush swelling and hysteresis. Thus, there remains a need for an experimental system that spans the full range of the ionizable monomer fraction to study the pH-dependent behavior of weak PEBs. Although, to the best of our knowledge, there are no theoretical models developed for random copolymeric weak PEBs, we posit that systems with a low ionizable monomer fraction will help inform theoretical predictions of weak PEBs.

To this end, we used surface-initiated copper(0) controlled radical polymerization (SI-CuCRP) to synthesize a series of random copolymer brushes with varying fractions of a weak basic monomer with good control over brush height, grafting density, and the fraction of the ionizable monomer. Using in situ ellipsometry and streaming zeta potential measurements, we study the effects of the ionizable monomer fraction on the state of ionization and swelling behavior of weak basic PEBs in response to changes in pH, encompassing both the highly charged and uncharged states. We find that varying f significantly affects the swelling behavior and hysteresis in PEBs, where the swelling ratio and the extent of hysteresis generally increase with increasing f, and propose that hydrophobicity at the brush periphery underlies the hysteresis in the swelling ratio.

EXPERIMENTAL SECTION

Materials. *Chemicals.* (3-Aminopropyl)triethoxysilane (APTES, 99%), triethylamine (TEA, ≥99.5%), α-bromoisobutyryl bromide (BiBB, 98%), *N*,*N*,*N*′,*N*″,*N*″-pentamethyldiethylenetriamine (PMDETA, 99%), tetrabutylammonium fluoride solution [TBAF, 1.0 M in tetrahydrofuran (THF)], and *N*,*N*-dimethylacetamide (DMA) were purchased from Sigma-Aldrich and used as received. 2-(Dimethylamino)ethyl acrylate (DMAEA, 98%) and 2-hydroxyethyl acrylate (HEA, 97%) were purchased from Thermo Scientific and passed through basic alumina columns to remove the inhibitor prior to use. Milli-Q grade deionized water was obtained from a Sigma Milli-Q water purification system (resistivity 18.2 MΩ·cm at 25 °C). Silicon wafers (p-doped, ⟨100⟩) were purchased from Addison Engineering. Copper plates were prepared by sputtering copper onto silicon wafers cut into 7.5 cm × 2.5 cm pieces (AJA ATC Orion Sputtering System).

Sample Preparation. Silicon wafers (7.5 cm × 2.0 cm) were sequentially sonicated in Milli-Q water, methanol, and acetone and subsequently dried under a nitrogen flow. Wafers were then surface activated via plasma treatment for 5 min (benchtop reactive ion etcher and plasma cleaner, PlasmaEtch Inc.). The plasma-treated wafers were placed inside a vacuum chamber alongside 0.2 mL of APTES for 1.5 h under static vacuum (<1 mbar) and then removed from the chamber and annealed for 1 h at 110 °C. This chemical vapor deposition (CVD) process results in a smooth APTES monolayer with a thickness of ≈0.6 nm and a root mean squared (rms) roughness of ≈0.2 nm. The annealed APTES-modified wafers were transferred to a glovebox operating under argon and placed inside a glass Petri dish containing 12 mL of anhydrous THF. TEA (0.55 mL, 0.3 M) was added to the solution, and lastly, BiBB (0.5 mL, 0.3 M) was added dropwise to the solution. The Petri dish was sealed and left to react for 1.5 h under argon, after which the initiator-modified wafers were rinsed with copious amounts of THF, methanol, and water and dried under nitrogen. The modified substrates were immediately used for polymerization or stored under a dry nitrogen environment at room temperature.

Brushes were prepared by SI-CuCRP, where a Cu(0) plate was used as an almost infinite source of copper ions.[25−27] A BiBB-modified Si wafer and a copper plate of the same size were attached, separated from each other by silicone spacers, and placed in a small custom reaction vessel. Reaction mixtures for different fractions were prepared by adding DMAEA and HEA in 100:0, 75:25, 50:50, 25:75, and 0:100 molar ratios to the solvent (water/methanol 2:1 vol/vol). The total concentration of monomers was set to 1.25 M for all fractions. PMDETA (40 mM) was added to the solution containing monomers and then thoroughly mixed. Within the reaction mixtures, DMAEA remains almost entirely neutral due to the basic pH of reaction mixtures (e.g., pH = 11.3 for $f = 1.00$). The reaction mixture was transferred to a custom vessel containing the BiBB-modified Si and copper plate and sealed with a rubber septum. After the specified reaction times (Table S1), the polymerization was quenched by removing the copper plate from the setup. The brush-modified surfaces were sequentially sonicated in acetone, methanol, and water to remove any adsorbed polymer or reagents and lastly were dried

https://doi.org/10.1021/acs.macromol.3c00947
Macromolecules 2023, 56, 9218−9228

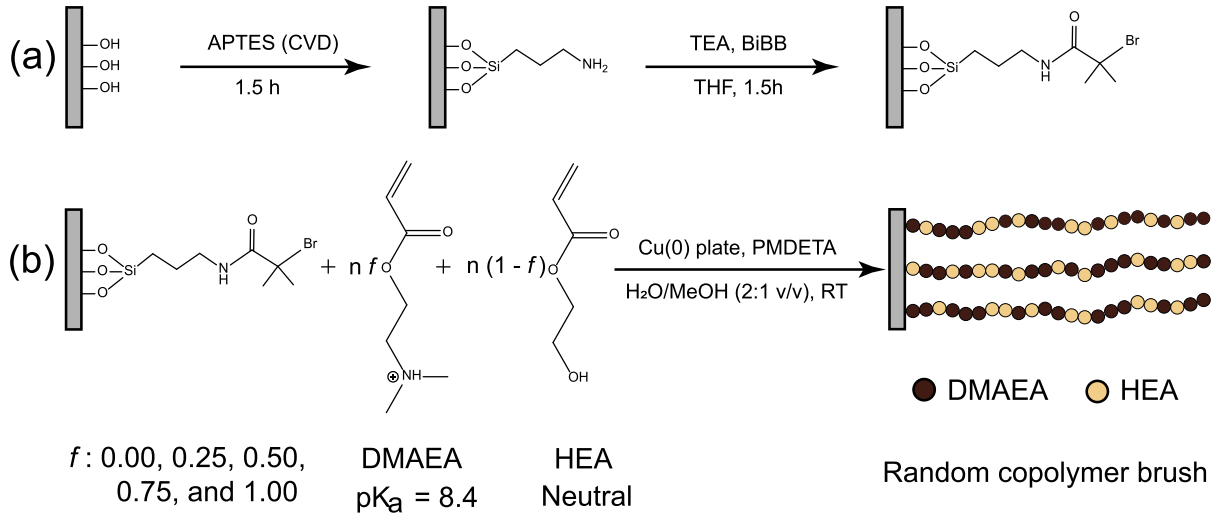

Figure 1. Process of brush synthesis: (a) two-step deposition of the ATRP initiator, where APTES is deposited by CVD and BiBB is attached to APTES under a dry Ar environment. (b) SI-CuCRP of brushes with the f fraction of DMAEA. DMAEA is depicted in the protonated form below its pK_a.

under a gentle nitrogen stream. The dried brush samples were stored in a dry nitrogen environment at room temperature.

Characterization. *X-ray Photoelectron Spectroscopy.* A PHI Quantera X-ray photoelectron spectrometer with a monochromatic Al Kα X-ray source was used to determine the monomer fraction in each brush sample. Survey spectra were taken at 140 eV. High-resolution spectra of O 1s, N 1s, and C 1s peaks were taken at 26 eV for 40, 30, and 30 sweeps with 0.05 eV steps, respectively. The high-resolution spectra were calibrated with respect to the C−C, C−H peak at 248.8 eV. Multipak software (Ulvac-Phi, inc.) was used to analyze the X-ray photoelectron spectroscopy (XPS) spectra.

Fourier Transform Infrared Spectroscopy. Fourier transform infrared (FTIR) spectra were taken with a Nicolet 6700 FTIR spectrometer (Thermo Fisher Scientific) in the attenuated total reflection (ATR-FTIR) mode with diamond as the crystal. Data were collected by performing 128 scans with an 8 cm^{-1} resolution. All spectra were analyzed with OMNIC software, where the ATR and baseline corrections were performed on the raw spectra.

Ellipsometry. An ellipsometer (M-2000S, J.A. Woollam, variable angle) equipped with a horizontal fluid cell (J.A. Woollam, a fixed angle of incidence of 75° and a volume of 5 mL) was used to measure the dry h_{dry} and wet h_{wet} thicknesses of the polymer brushes. The acquired spectra were analyzed using WVASE32 software. In the dry state, brushes were measured at multiple angles (65, 70, and 75°), and the data were fit with a Cauchy model, $n(\lambda) = A + B/\lambda^2$, for brush thickness and the first two Cauchy parameters, A and B. In the swollen state, a 50 mL exchange volume and 30 min equilibration time were used to ensure a steady state at a given pH. The pH values were set by adding either 0.1 M HCl or NaOH to nonbuffered Milli-Q water. This method resulted in negligible pH drifts during the experiments. Depending on the brush thickness, two models were used to analyze the in situ ellipsometry results. For brushes with swollen thicknesses up to ≅150−180 nm, data were fit with a Cauchy model for brush thickness and first and second Cauchy parameters (a total of three fit parameters) with a water ambient layer. For thicker brushes, an effective medium approach (EMA)-based graded model was used.[28,29] This model describes the continuous variation of the sample refractive index normal to the substrate. The swollen brush was divided into two main layers, with each sliced into multiple sublayers. The polymer was represented by a Cauchy model, where the parameters obtained from the dry brush measurements were set as constants and data were fit for the brush thickness, middle node position, and polymer fraction in two EMA layers with the remainder water (a total of four fit parameters for the entire brush).

Streaming Zeta Potential. The surface zeta potential of the brushes was measured by using an electrokinetic analyzer with an adjustable gap cell (SurPASS 3, Anton Paar). A 1 mM KCl electrolyte solution was streamed through a 100 μm wide slit channel between two 1 × 2 cm^2 brush samples. The concentration of the KCl solution was chosen to minimize the effect of the sample surface conductance. The pH of the nonbuffered KCl aqueous solution was varied stepwise with an auto pH titration between 3.0 and 10.0 by adding 50 mM HCl or NaOH solutions. At a given pH, brushes were rinsed three times with 100 mL of the electrolyte solution before measurement, and the average of three measurements was reported as the zeta potential value. The charge separation between the inlet and outlet of the cell induced by the shear forces acting on counterions leads to an electrical potential difference (streaming potential), which is detected as a direct current (DC) voltage. The zeta potential is then determined from the measured streaming potential using the Helmholtz−Smoluchowski (HS) equation $\zeta = \frac{dU_{str}}{d\Delta P} \times \frac{\eta}{\epsilon \times \epsilon_0} \times \frac{L}{A} \times \frac{1}{R}$, where η is the viscosity, ϵ is the dielectric coefficient of the electrolyte solution, ϵ_0 is the permittivity, L = 2 cm is the length of the rectangular slit channel, $A \approx 0.01$ cm^2 is the area of the channel cross-section, and R is the electrical resistance inside the streaming channel.[30]

RESULTS AND DISCUSSION

Characterization of Brushes with Various Fractions of the Ionizable Monomer. To investigate the role of the ionizable monomer fraction f on the pH-dependent swelling behavior of PEBs, we synthesized a series of random copolymer brushes using SI-CuCRP[27] with varying fractions of DMAEA to HEA monomers from f = 1.00 to f = 0.00 in f = 0.25 decrements, where f represents the fraction of DMAEA in the PEBs (Figure 1). All fractions maintained linear reaction kinetic profiles (Figure S1) up to ≃75 nm dry thickness h_{dry}, indicating good control over the polymerization reactions.[31,32] This large dry brush thickness enables direct comparisons to current PEB theories.[14]

The fractions of DMAEA monomers in the brush samples were measured by using XPS. High-resolution spectra show that the N 1s peak intensity increases concomitant with f, qualitatively verifying an increase in the fraction of DMAEA monomers (Figure 2a). The ratio of O 1s/C 1s orbitals was used to quantitatively measure the f values (details on

https://doi.org/10.1021/acs.macromol.3c00947
Macromolecules 2023, 56, 9218−9228

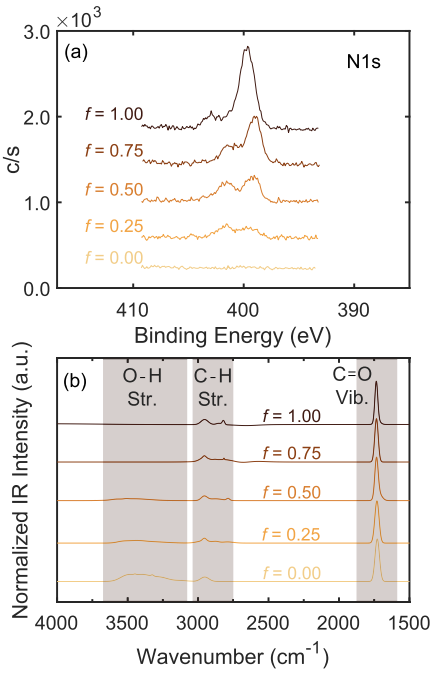

Figure 2. (a) High-resolution XPS spectra of N 1s orbital of brushes with a thickness of ≈75 nm. (b) ATR-FTIR spectra of brushes with C═O vibrational and C−H and O−H stretching peaks highlighted.

calculations and high-resolution spectra of O 1s and C 1s orbitals in the Supporting Information), which are observed to closely follow the initial monomer ratios in the reaction mixture. However, XPS probes the first 1−10 nm off of the surface.[33,34] To measure the fraction of DMAEA throughout the brush depth, we cleaved the brushes in a stepwise fashion with 0.1 M solution of TBAF in DMA. This process decreased grafting density, resulting in chain collapse and decreasing brush thickness. XPS measurements show that the composition of elements remains relatively constant throughout the entire brush for all fractions, indicating that the monomers are distributed in a truly random fashion, with no evidence of block or gradient copolymer formation (see the discussion on the effect of reactivity ratios (r_i) in the Supporting Information). The average value of all depths was used as the true f value of the brushes (Table 1). ATR-FTIR

Table 1. Brush Properties

f_{synth}	h_{dry} (nm)[a]	f_{XPS}	σ (nm^{-2})[b]
1.00	76 ± 1	1.00 ± 0.00	0.10−0.16
0.75	78 ± 1	0.75 ± 0.01	0.24−0.32
0.50	73 ± 2	0.47 ± 0.02	0.27−0.35
0.25	74 ± 2	0.26 ± 0.02	0.22−0.30
0.00	78 ± 1	0.00 ± 0.00	0.23−0.30

[a]The standard deviation is calculated from measurements of at least 5 points. [b]The lower and upper bounds correspond to ν = 0.50 and 0.60, respectively.

measurements show a gradual decrease in the −OH stretch peak (only present in HEA), a change in the shape of the C−H stretch peak, and a shift in the carbonyl vibrational peak (Figure S5) as f is increased, all qualitatively corroborating the XPS measurements (Figure 2b). Since the measured values of f for all fractions are close to their initial stoichiometric values, we will hereafter refer to the brushes by these values.

We used the swelling method to verify that our surface grafted polymers have comparable grafting densities and are in the brush regime. Due to the poor refractive index contrast and little amount of the polymer obtained from cleaving brushes, a direct measurement of molecular weight M_n and grafting density was not feasible. For systems where grafting density cannot be directly measured, the swelling method has been successfully used to estimate and track changes in the grafting density.[25,35−37] We measured brush heights in the dry state and in good solvent conditions (acetone) for all fractions using ellipsometry and calculated the grafting density using the Alexander−de Gennes brush model.[38,39] Here, the swelling ratio α_{SR} can be related to grafting density

$$\sigma = a^{-2}\alpha_{SR}^{\frac{2\nu}{1-3\nu}},\ \alpha_{SR} = \frac{h_{wet}}{h_{dry}} \quad (1)$$

where h_{wet} and h_{dry} are the swollen (in acetone) and dry brush thickness (both determined by ellipsometry), respectively, a is the segment length of the chains, calculated from the monomer molar volume,[40] and ν is the Flory exponent. The calculated σ from eq 1 is highly dependent on ν. Because PDMAEA is more solvated in acetone than PHEA, using a typical value of ν = 0.6 for all fractions may be erroneous. Moreover, it has been reported that at high grafting densities, brushes are better described as Gaussian blobs, similar to polymer chains in a theta solvent, such that ν will have a value close to 0.5.[41,42] Considering these two uncertainties, we report a range of σ values from ν (0.50−0.60). The true σ values for all samples are expected to fall within these limits. The physical properties of the brushes are summarized in Table 1. Although reaction conditions were kept the same for all fractions (Supporting Information), the grafting density for f = 1.00 is somewhat smaller than that of the other fractions. We speculate that this could be due to the larger size and faster rate of polymerization and quenching for DMAEA than that for HEA, resulting in a lower grafting density. Overall, the grafting densities for all charge fractions fall within the brush regime and allow direct comparisons of pH-dependent brush properties.

Swelling of the PDMAEA Brush. In situ ellipsometry was used to measure the pH-responsive behavior of brushes as a function of the charge fraction. Initially, we investigated the swelling behavior of the f = 1.00 brush from pH 3.0 to pH 10.0 in the forward direction and from pH 10.0 to pH 3.0 in the backward direction. The brush height is responsive to pH changes with the maximum and minimum swelling ratios at pH values of 3.0 and 10.0, respectively (Figure 3). The swelling ratio gradually decreases in the forward direction, which differs from the sharp change in chain conformation observed around the pK_a for weak polyelectrolytes in solution.[43−46] This behavior is attributed to nonuniform ionization along the brush chains, where α exponentially decays as a function of brush depth; the superficial monomers can gain or lose charge more readily than those deeper in the brush.[13,17,18] As a result, the basic groups in the brush are expected to have a range of pK_a values, and the average pK_a values of all basic groups along a brush (apparent pK_a) can be determined from the inflection point of the ionization curve of the brushes.

From the swelling curves, we extract the transition pH, pH*, defined as the pH value at which the swelling ratio curve reaches its inflection point, by fitting the swelling curves to a sigmoidal function (details on the fit functions can be found in the Supporting Information).[23] As the degree of ionization α

https://doi.org/10.1021/acs.macromol.3c00947
Macromolecules 2023, 56, 9218−9228

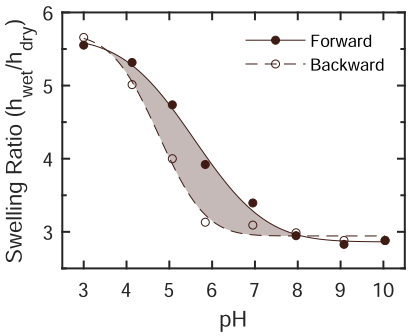

Figure 3. Swelling ratio h_{wet}/h_{dry} (ratio of the solvated h_{wet} to dry h_{dry} brush thickness) of the PDMAEA brush as a function of pH in deionized water. The pH was first increased from 3.0 to 10.0 (closed symbols, solid line) in the forward direction and then decreased from 10.0 to 3.0 (open symbols, dashed line) in the backward direction. The shaded area between the curves represents the extent of hysteresis.

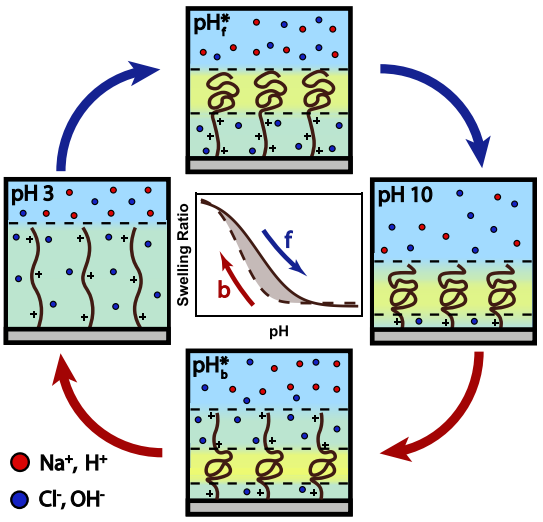

Figure 4. Hydrophobic periphery mechanism causing an acid shifted hysteresis in the backward direction. In the forward direction, the periphery forms and increases in size, causing a wide pH-responsiveness range. In the backward direction, the periphery shifts the response to more acidic values. The green and yellow parts represent charged hydrophilic and neutral hydrophobic regions of the brush, respectively.

drives the brush swelling behavior, pH* can be used as an approximation for the apparent pK_a of the brush. In the forward direction, the $f = 1.00$ brush has a $pH_f^* = 5.6$, which is approximately 3.0 units smaller than the pK_a of the DMAEA monomer (pK_a = 8.4).[47] Similar shifts in apparent pK_a have been observed for other weak PEBs and are attributed to confinement effects in the brush that cause the amine groups to behave as weaker bases than the free monomer.[48,49]

In the backward direction, the minimum and maximum values of the swelling curves are the same as those measured in the forward direction. These values are in good agreement with prior measurements on brushes that contain the methacrylate analogue of DMAEA (poly[(2-dimethylamino)ethyl methacrylate)] (PDMAEMA) with similar dry thickness, indicating that SI-CuCRP results in grafting densities similar to other SI-ATRP techniques.[28,35] Interestingly, in the intermediate pH range, the response in the backward direction is hysteretic, shifting toward more acidic pH values with $pH_b^* = 4.8$ (Figure 3). It has been previously postulated that the formation of a hydrophobic periphery causes the hysteretic behavior observed in the pH-dependent swelling behavior.[48,50] Figure 4 represents schematically the mechanistic details of this hysteretic behavior. In the forward direction, at pH values below $pH_f^* = 5.6$, the tertiary amine groups are highly protonated, resulting in a larger concentration of hydroxide and chloride ions (from the added HCl) in the brush layer than that in the bulk solution. The imbalance between the concentration of hydroxide and chloride ions in the brush and the bulk exerts a large osmotic pressure difference between these two regions that significantly swells the brush (i.e., strongly charged osmotic brush regime).[13,51] As the pH increases, the amine groups adjacent to the bulk phase deprotonate first to form a neutral, hydrophobic periphery at the brush surface[29,50] (Figure 4). The thickness of this hydrophobic periphery increases with pH and slows the uptake of water and ions into the brush layer, therefore increasing the range of pH-responsive behavior. Beyond pH 8.0, the swelling ratio remains fairly constant, indicating that the brush is no longer pH-responsive. We posit that at this pH, the hydrophobic periphery reaches a critical thickness that blocks further adsorption of water and ions into the brush, thus preventing additional deprotonation. In addition, due to the absence of added salt in our systems, some amine groups remain protonated below the hydrophobic periphery.[48,49] In the backward direction, decreasing the pH allows the amine groups at the upper surface of the brush to get protonated. However, the remainder of the hydrophobic periphery hinders protonation of the deeper layers of the brush. Thus, compared to the forward direction, a more acidic pH is required to achieve a similar degree of protonation, which shifts the response to more acidic values ($pH_b^* = 4.7$). As pH is further decreased, the hydrophobic periphery gradually shrinks in size, and eventually, at pH 3.0, we recover the initial swelling in the forward direction. The hydrophobic periphery mechanism is a kinetic effect as it depends on the rate of water and ion uptake between the brush and the bulk and on the relaxation times of chains due to swelling/deswelling in response to changes in pH. The extent of hysteresis decreases with time and eventually reaches the steady states of Figure 3. Based on our control experiments, we have discarded the effects of the hydrolysis of DMAEA on the observed swelling behavior. (See the discussion on the extent of hydrolysis in the Supporting Information.)

Effects of the Ionizable Monomer Fraction on Swelling. Next, we investigated the influence of the fraction of ionizable monomers on the pH-dependent swelling behavior of PEBs. All fractions display pH-dependent swelling behavior, barring $f = 0.00$, which does not possess any ionizable groups (Figure 5). Similar to $f = 1.00$, all fractions containing ionizable monomers ($f > 0$) display maximum and minimum swelling ratios at acidic and basic pH values, respectively, regardless of the direction (i.e., forward versus backward). The maximum and minimum swelling ratios, however, depend on f. First, the maximum swelling ratio decreases as f decreases. At this pH, in the absence of added salt, the amine groups are strongly charged and all weak PEB charge fractions behave similarly to strong PEBs in the osmotic brush regime,[10,13,52] where the swollen brush thickness is independent of grafting density and charge effects are the main driving force for swelling.[10,11] This idea is further evidenced by the fact that the grafting density of

https://doi.org/10.1021/acs.macromol.3c00947
Macromolecules 2023, 56, 9218−9228

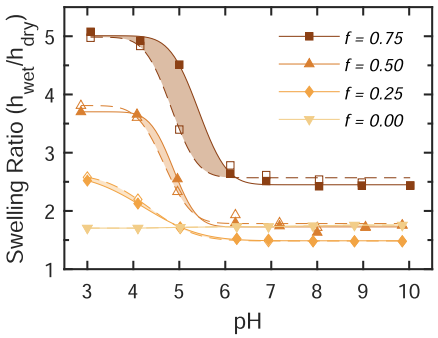

Figure 5. Swelling ratio of PEB fractions as a function of pH in DI water. pH was first increased from 3.0 to 10.0 (solid lines) and then decreased from 10.0 to 3.0 (dashed lines). The shaded areas represent the extent of hysteresis.

f = 1.00 is nearly half the value of the other fractions, yet the swelling ratio directly follows the trend with f. At acidic pH values, the superficial DMAEA groups behave similarly in terms of protonation regardless of their f values, as is evident from the narrow pH range of 3.0−4.0 where the maximum α_{SR} plateau occurs for all charge-containing brushes. We note that we define f as the fraction of ionizable monomers, whereas in theories, for strong PEBs, f is the degree of ionization α. In a weak PEB, α is influenced by proximity to the apparent pK_a of the brush and does not necessarily equal f.[10,11,13,52] However, pH 3.0 is well below the pH* of all charge fractions (discussed further below), and it can be assumed that amine groups are maximally protonated, and f follows the trends of α. Overall, as f is decreased, the osmotic pressure difference decreases, resulting in lower swelling ratios.

Contrary to the maximum swelling ratio, the minimum swelling ratio has a nonmonotonic trend with f, first decreasing from f = 0.00 to f = 0.25 and then increasing up to f = 1.00 (Figure 6). The minimum swelling ratio is measured at pH

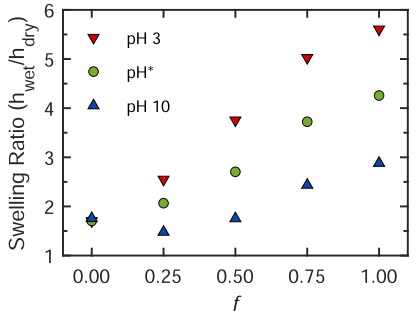

Figure 6. Effects of varying the DMAEA fraction (f) on the swelling behavior of brushes at pH 3.0 and pH 10.0 and at the transition pH* of the forward and backward cycles. The values at pH 3.0 and pH 10.0 are the average of the swelling ratios in both directions. pH* is determined from the inflection point of sigmoidal fits to the data.

10.0, where all brushes are expected to be almost entirely neutral. Therefore, the chemistry of the neutral monomer will begin to dominate the swelling behavior. Because HEA is more hydrophilic than DMAEA, as evidenced from contact angle measurements,[27] it is expected for the swelling ratio to decrease as f is increased, with the exception of f = 1.00, which has a lower grafting density and is expected to have a higher swelling ratio in the neutral state.[39,53] In contrast to this expectation, we observe an increase in the swelling ratio as f increases from 0.25 to 1.00, indicating that the hydrophobicity of DMAEA is not the sole factor determining the swelling behavior. Previous studies have shown that at extremely low ionic strengths, homopolymeric weak polybasic brushes are not easily deprotonated at pH values above their apparent pK_a and/or pH*.[48,49,54] Under our experimental conditions (deionized water with no added salt), the ionic strength is solely determined by the amount of added acid or base, and we expect weak PEBs with higher f to have a non-negligible number of protonated groups, which even at pH 10.0 can dominate the swelling behavior. As f decreases, the net number of ionizable groups decreases, and as a result, the number of protonated groups at pH 10.0 decreases. For f = 0.50 and f = 0.25, the electrostatic effects due to the remaining protonated groups become comparable (and possibly less significant, for f = 0.25) to the hydrophobic interactions, resulting in the observed nonmonotonic trend. As the pH is decreased, electrostatic interactions again dominate, and for the swelling ratio at pH*, a monotonic trend in the swelling ratio with f is recovered. As our pH range covers both minimum and maximum swelling ratio plateaus, the swelling ratio values at pH* (the inflection point of the curves) coincide with the average of the minimum and maximum swelling ratios. The trends shown in Figure 6 further support the proposed pH-dependent swelling mechanism discussed in Figure 4, where even above pH*, protonated groups are still present.

Additionally, we performed in situ atomic force microscopy (AFM) measurements on brushes with f = 0.00, 0.50, and 1.00 at pH ≈ 3, 6, and 10 (Figure S20) to determine swelling ratios using a model-independent method. The results from AFM measurements are in good agreement with the ellipsometry measurements and confirm the pH-dependent swelling behavior as a function of the ionizable monomer fraction (Figure S21 and Table S6).

We examine the influence of f on pH* in the forward direction. As f decreases, the swelling response of the brushes shifts to more acidic values, with pH* decreasing from pH_f^* = 5.6 for f = 1.00 to pH_f^* = 4.2 for f = 0.25 (Table 2). Moreover,

Table 2. pH at Transition pH* for All Fractions in the Forward pH_f^* and Backward pH_b^* Directions[a]

f	pH_f^*	pH_b^*
1.00	5.6 ± 0.1	4.7 ± 0.2
0.75	5.4 ± 0.2	4.8 ± 0.2
0.50	4.9 ± 0.1	4.7 ± 0.2
0.25	4.2 ± 0.1	4.3 ± 0.1

[a]The error associated with each value is determined from the fitting errors.

the pH where the minimum in the swelling ratio occurs shifts to more acidic values as f decreases, therefore narrowing the range of pH-responsiveness. We attribute this acidic shift to the lower number of amine groups present as f decreases. By introducing the neutral HEA monomers, at mid to low pH values (pH* to pH 3.0), the hydrophobic character of the brush increases with decreasing f. The higher hydrophobicity of the brush results in a more hydrophobic periphery[48] that reaches its critical thickness at more acidic pH values, therefore shifting and narrowing the range of pH-responsiveness to more acidic values as f decreases.

Hysteretic behavior is observed for all fractions containing ionizable monomers, with the extent of hysteresis (shaded

https://doi.org/10.1021/acs.macromol.3c00947
Macromolecules 2023, 56, 9218−9228

areas of Figures 3 and 5) decreasing with decreasing f. We find that the pH* in the backward direction shifts to more acidic values for f = 0.75 and 0.50 and that the difference between the forward and backward direction narrows with decreasing f (Table 2). The pH* of the f = 0.25 brush in the backward direction has a slightly larger value than in the forward direction, which is possibly due to the negligible extent of hysteresis in this brush and the errors associated with in situ ellipsometry measurements. Similar to the f = 1.00 brush, we hypothesize that the hysteresis in the intermediate pH range is a result of differing degrees of protonation in the forward and backward directions caused by the formation of the hydrophobic periphery (Figure 4). As f decreases, the number of groups that are able to get protonated decreases and the difference in the degree of protonation between the forward and backward directions becomes smaller, resulting in a lower extent of hysteresis and a smaller difference between the pH* values for both directions. A similar trend has been previously reported for statistical random copolymer brushes of 2-(diethylamino)ethyl methacrylate (DEA), a weak base, and 2-(2-methoxyethoxy)ethyl methacrylate (MEO_2MA), a temperature-responsive neutral monomer.[23] In that study, it was shown that the pH* shifted to more acidic pH values as the DEA fraction was decreased from f = 0.50 to f = 0.10 at a fixed temperature. The response in the opposite direction was also hysteretic and further shifted toward acidic pH values. Further, they performed numerical self-consistent field theory (nSCFT) calculations, which closely resemble the general trends of our data, especially in the highly protonated regime. However, in their experiments, they found a nonmonotonic trend between f and swelling ratio at acidic pH values. In our work, we have explored a wider range of ionizable monomer fractions with monomers of similar size, which could be the reason for a better match of our data to nSCFT calculations.

Charge State of Brushes. To directly probe the charge state of the brush, we measured the streaming zeta potential of the PEBs. Zeta potential ζ is the electrical potential at the shear plane of an electric double layer and is a measure of the effective charge of a surface in contact with a solution.[55] Figure 7 shows ζ as a function of pH for all brushes containing ionizable monomers. At pH values below the apparent pK_a of the brush, the amine groups are protonated and bear a positive charge. In this regime, the ζ−pH curve of the f = 1.00 brush exhibits a plateau in both directions, indicating that the formation of the electric double layer is mainly caused by the protonation of the basic groups.[56] As the pH is further decreased from pH 4 to pH 3, the zeta potential increases from the plateau. We believe that this increase is due to the increased ionic strength (from ≈1 mM at pH 4 to ≈2 mM at pH 3) and an excess of hydronium ions adsorbed to the double layer. As pH is increased in the forward direction, the basic groups gradually lose their charge, leading to a decrease in zeta potential, and finally, at around pH ≈ 9.5, another plateau is reached. The negative ζ values at basic pH conditions arise from the increase in brush hydrophobicity, which leads to water molecules being replaced by hydroxide ions at the brush surface.[57] Similar to the swelling ratio curves, the ζ−pH curves also show a large range of pH-responsiveness, caused by the nonuniform ionization along PEB chains.

The shapes of the ζ−pH curves change with f. As f decreases, the plateau under acidic conditions gradually disappears. Nevertheless, the plateau at basic pH values remains for all PEBs. Furthermore, the values of ζ are dependent on f, where the values of ζ at the acidic (pH 4.0) and basic (pH 9.5) plateaus increase as f increases, consistent with the increasing number of ionizable groups in the PEBs (Figure 8a). These results corroborate the in situ ellipsometry measurements (Figure 6) and verify our hypothesis that brushes with higher f values have larger osmotic pressure differences due to a larger number of protonated amine groups (Figure 8a). In addition, under basic pH conditions, ζ values decrease as f is decreased and the minimum ζ is achieved for f = 0.25, which is in accord with our hypothesis that hydrophobic interactions dominate the conformation of the PEBs with smaller f ($f \leq 0.50$) under basic pH conditions.

From the ζ−pH curves, the isoelectric point (pI) can be determined, which is a measure of the apparent pK_a of the PEBs.[58,59] Decreasing f results in a decrease in the pI and thus the apparent pK_a of PEBs (Figure 8b). This trend is consistent with the calculated pH* from in situ ellipsometry measurements, yet the values are widely different (Table 3). We believe that this difference is mainly due to the presence of an added

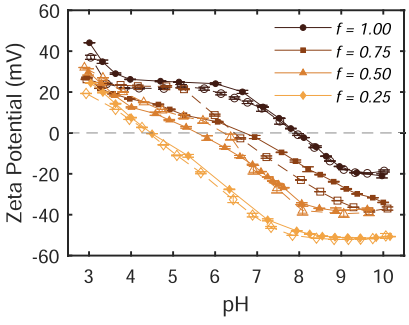

Figure 7. Zeta potential ζ of random copolymer brushes of DMAEA and HEA with various fractions of charged groups f as a function of pH in a 1 mM KCl solution. pH was first increased from 3.0 to 10.0 (closed symbols, solid lines) and then decreased from 10.0 to 3.0 (open symbols, dashed lines). The intersection of the dashed line and the curves determines the isoelectric point (pI) of the brushes.

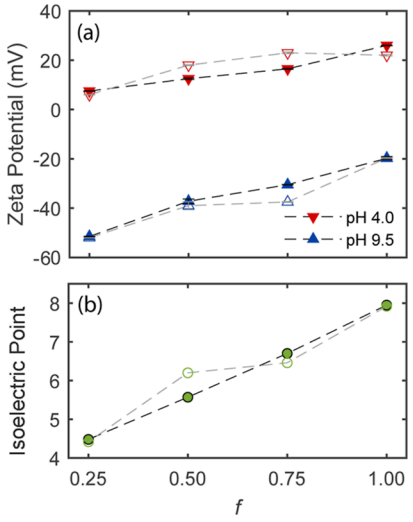

Figure 8. (a) Zeta potential at acidic (pH 4.0) and basic (pH 9.5) pH values and (b) isoelectric point (pI) decrease with f in both directions. Error for all measurements is below 1% and is the standard deviation of three measurements per pH value on a single sample. Closed and open markers represent forward and backward directions, respectively.

https://doi.org/10.1021/acs.macromol.3c00947
Macromolecules 2023, 56, 9218−9228

Table 3. pH at Transition pH* and Isoelectric Point pI for All Fractions in the Forward and Backward Directions[a]

f	pH_f^*	pI_f	pH_b^*	pI_b
1.00	5.6 ± 0.1	7.9 ± 0.1	4.7 ± 0.2	7.9 ± 0.1
0.75	5.4 ± 0.2	6.7 ± 0.1	4.8 ± 0.2	6.5 ± 0.1
0.50	4.9 ± 0.1	5.6 ± 0.1	4.7 ± 0.2	6.2 ± 0.1
0.25	4.2 ± 0.1	4.5 ± 0.1	4.3 ± 0.1	4.4 ± 0.1

[a]Reported error is calculated from the fit functions.

salt (1 mM KCl) that is necessary for the proper formation of the electric double layer. Previous studies have shown that the addition of monovalent salts, even at concentrations decades below the crossover concentration, can facilitate the protonation of weak PEBs by screening the repulsion between ionizable groups within the brush and reducing the free energy cost of protonation. This easier protonation effectively shifts the apparent pK_a to more basic pH values.[14,49,51] In addition, our results show that as f decreases, the difference between pH* and pI becomes smaller. At low f, the repulsive forces between brush chains are weaker, and thus, charge screening effects and the difference between the two salt conditions become less significant, resulting in a smaller difference between the values of pH* and pI (Table 3).

Similar trends are present in the backward direction, with ζ increasing as pH is decreased and f is increased. However, the ζ−pH curves exhibit negligible hysteresis between the forward and backward directions (Figure 7), in contrast to the pronounced hysteresis observed using in situ ellipsometry (Figures 3 and 5). Although the curves of the backward direction do not fall on the forward curves, this inconsistency between the two directions does not follow any trends with f or pH values. For instance, for the f = 1.00 brush, the curves are identical from pH 10.0 to pH 7.0 but deviate at more acidic pH values. As a result, the values of pI and ζ at pH 9.5 are the same in both directions, while the values of ζ at pH 4.0 are slightly different (Figure 8a). This nonordered difference between the two directions is inconsistent with hysteretic behavior, and we believe that the differences between the two directions are possibly due to the errors associated with zeta potential measurements. A control experiment on a bare silicon surface, where no hysteresis between the two directions is present, showed a similar nonordered inconsistency between the forward and backward directions, supporting the idea that the differences are due to instrumental error (Figure S8).

The absence of hysteretic behavior cannot be justified by the presence of salt in the streaming zeta potential measurements. In fact, weak PEBs have been shown to experience hysteresis in the presence of different concentrations of added salt.[29] We posit that the absence of hysteresis is due to the length scales probed in the streaming zeta potential measurements. The length of the shear plane (the probing length of zeta potential measurements) is believed to be of the same order of magnitude of the Debye length of the solution.[60−62] The Debye length for the zeta potential measurements, $\lambda \approx 5$ nm, is 2 orders of magnitude smaller than the thickness of swollen brushes probed with ellipsometry. Figure 9 depicts these differences schematically, where the ratio of probing length for ellipsometry L_e to the swollen thickness h_e is $L_e/h_e = 1$ and the ratio of probing length for zeta potential L_z to the swollen thickness under flow h_z is $L_z/h_z \ll 1$. This hypothesis ($L_z/h_z \ll 1$) may suggest another reason for the differences between pI and pH* values as the superficial basic groups probed in zeta potential measurements have larger pK_a values. However, it has been shown that brushes collapse under fluid flow, causing their swollen thickness to be smaller than the swollen thickness measured with ellipsometry.[63−65] This hypothesis requires $L_z/h_z \ll 1$ to obtain a significant difference between the two measurements, and further experiments under flow and in the presence of salt are required to verify it, which we will address in a future publication.

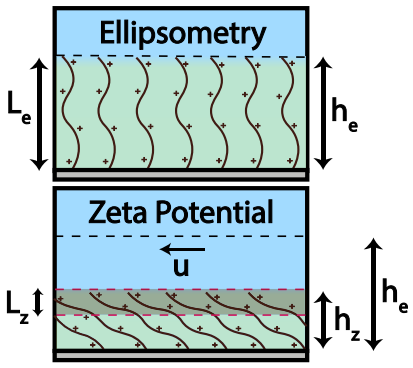

Figure 9. Cartoon depicting the different length scales probed in ellipsometry and streaming zeta potential measurements. In ellipsometry, the probing length L_e is equal to the swollen thickness h_e. In zeta potential measurements, due to the liquid flow (at a constant velocity u), brushes stretch in the planar direction and collapse, causing the swollen thickness in zeta potential measurements h_z to be smaller than h_e. The probing length of zeta is $L_z \approx 5$ nm, orders smaller than those of h_e and possibly h_z.

CONCLUSIONS

We investigated the swelling and ionization behavior of weak PEBs with varying fractions of ionizable monomers f using in situ ellipsometry and zeta potential measurements. SI-CuCRP was used to synthesize well-controlled weak PEBs consisting of varying fractions of DMAEA (weak base) and HEA (neutral hydrophilic) monomers, verified by XPS and ATR-FTIR spectroscopy.

In situ ellipsometry measurements showed that all charge containing brushes exhibited pH-responsive behavior, with the maximum and minimum swelling ratios occurring at acidic and basic pH, respectively. We showed that the maximum swelling ratio increased with increasing f, in agreement with the nSCFT prediction for highly charged weak osmotic brush behavior in the absence of salt. The minimum swelling ratio also increased with increasing f. We propose that hydrophobic interactions dominate brush conformation at low f values, resulting in a nonmonotonic trend in the swelling ratio. The swelling behavior in the backward direction was hysteretic and generally shifted the pH-responsive behavior to more acidic pH values. The extent of this hysteresis decreased with decreasing f, such that the hysteresis became negligible at f = 0.25. The brush composition/architecture affects the extent of hysteresis but does not appear to be its origin. All of the observed trends are in agreement with the hypothesized hydrophobic periphery mechanism proposed for homopolymer brushes[48,50] and the nonuniform distribution of charge in weak PEBs.

Streaming zeta potential measurements show trends similar to those of the brush swelling ratio with both pH and f at acidic and basic pH values. However, the absolute value of pI, measured from the streaming zeta potential, was consistently larger than the pH* measured from ellipsometry, with the

https://doi.org/10.1021/acs.macromol.3c00947
Macromolecules 2023, 56, 9218−9228

difference narrowing with decreasing f. Moreover, no ordered hysteresis between the backward and forward cycles was observed. We hypothesize that these discrepancies are due to the presence of salt in the zeta potential measurements and differences in the probing depth between the two measurements. Whereas ellipsometry probes the whole depth of the brush, zeta potential is localized to the superficial layers where the basic groups can more readily gain and lose charge. Thus, the local pK_a is larger than the apparent pK_a of the brushes and their behavior is nonhysteretic.

Our study demonstrates that the fraction of ionizable monomers significantly affects the conformation and pH-responsive behavior of weak PEBs. We anticipate that neutron reflectivity measurements on PEBs at appropriate length scales will likely provide further insights into the effect of the ionizable monomer fraction on the monomer density distribution normal to the surface, as well as the distribution of co-ions. In addition, our platform enables future investigations on the effects of grafting density, weak versus strong polyelectrolytes, and salt concentration. We posit that our system may be used to test and inform the weak polyelectrolyte theory that assumes charge fractions $\ll 1$.[13,52] Further, the fraction of ionizable monomers provides another parameter to tune the stimulus response of surfaces for applications in separations and antifouling coatings.

■ ASSOCIATED CONTENT

Supporting Information

The Supporting Information is available free of charge at https://pubs.acs.org/doi/10.1021/acs.macromol.3c00947.

XPS spectra, FTIR spectra, AFM topographs, and reaction kinetics measurements, as well as detailed synthesis and fitting protocols (PDF)

■ AUTHOR INFORMATION

Corresponding Authors

Jacinta C. Conrad − *Department of Chemical and Biomolecular Engineering, University of Houston, Houston, Texas 77204, United States;* orcid.org/0000-0001-6084-4772; Email: jcconrad@uh.edu

Amanda B. Marciel − *Department of Chemical and Biomolecular Engineering, Rice University, Houston, Texas 77005, United States;* orcid.org/0000-0001-9403-396X; Email: am152@rice.edu

Authors

Shahryar Ramezani Bajgiran − *Department of Chemical and Biomolecular Engineering, Rice University, Houston, Texas 77005, United States;* orcid.org/0009-0007-9223-3838

Farshad Safi Samghabadi − *Department of Chemical and Biomolecular Engineering, University of Houston, Houston, Texas 77204, United States;* orcid.org/0000-0003-0556-000X

Si Li − *Department of Chemical and Biomolecular Engineering, University of Houston, Houston, Texas 77204, United States;* orcid.org/0000-0001-6579-2916

Complete contact information is available at: https://pubs.acs.org/10.1021/acs.macromol.3c00947

Notes

The authors declare no competing financial interest.

■ ACKNOWLEDGMENTS

We thank the Shared Equipment Authority at Rice University for access to the XPS, FTIR, and Sputtering system. We further thank Prof. Vincent Donnelly for access to the ellipsometer, Prof. Devin Shaffer for access to streaming zeta potential, and Prof. Rimer for access to the atomic force microscope. We thank the National Science Foundation (CBET-2113769 and CBET-2113767 to J.C.C. and A.B.M., respectively) and the Welch Foundation (E-1869 and C-2003-20190330 to J.C.C. and A.B.M., respectively) for partial support of this work.

■ REFERENCES

(1) Zhao, C.; Li, L.; Wang, Q.; Yu, Q.; Zheng, J. Effect of film thickness on the antifouling performance of poly (hydroxy-functional methacrylates) grafted surfaces. *Langmuir* **2011**, *27*, 4906−4913.

(2) Higaki, Y.; Kobayashi, M.; Murakami, D.; Takahara, A. Anti-fouling behavior of polymer brush immobilized surfaces. *Polym. J.* **2016**, *48*, 325−331.

(3) Khakzad, F.; Dewangan, N. K.; Li, T.-H.; Safi Samghabadi, F.; Herrera Monegro, R.; Robertson, M. L.; Conrad, J. C. Fouling Resistance and Release Properties of Poly (sulfobetaine) Brushes with Varying Alkyl Chain Spacer Lengths and Molecular Weights. *ACS Appl. Mater. Interfaces* **2023**, *15*, 2009−2019.

(4) Borukhov, I.; Leibler, L. Stabilizing grafted colloids in a polymer melt: Favorable enthalpic interactions. *Phys. Rev. E* **2000**, *62*, R41−R44.

(5) Tairy, O.; Kampf, N.; Driver, M. J.; Armes, S. P.; Klein, J. Dense, highly hydrated polymer brushes via modified atom-transfer-radical-polymerization: structure, surface interactions, and frictional dissipation. *Macromolecules* **2015**, *48*, 140−151.

(6) Zhang, R.; Ma, S.; Wei, Q.; Ye, Q.; Yu, B.; Van Der Gucht, J.; Zhou, F. The weak interaction of surfactants with polymer brushes and its impact on lubricating behavior. *Macromolecules* **2015**, *48*, 6186−6196.

(7) Zheng, H.; Wang, C.; Pavase, T. R.; Xue, C. Fabrication of copolymer brushes grafted superporous agarose gels: Towards the ultimate ideal particles for efficient affinity chromatography. *Colloids Surf., B* **2022**, *217*, 112705.

(8) Nagase, K.; Sakurada, Y.; Onizuka, S.; Iwata, T.; Yamato, M.; Takeda, N.; Okano, T. Thermoresponsive polymer-modified microfibers for cell separations. *Acta Biomater.* **2017**, *53*, 81−92.

(9) Wu, T.; Efimenko, K.; Vlček, P.; Šubr, V.; Genzer, J. Formation and properties of anchored polymers with a gradual variation of grafting densities on flat substrates. *Macromolecules* **2003**, *36*, 2448−2453.

(10) Pincus, P. Colloid stabilization with grafted polyelectrolytes. *Macromolecules* **1991**, *24*, 2912−2919.

(11) Israels, R.; Leermakers, F.; Fleer, G. J.; Zhulina, E. B. Charged polymeric brushes: Structure and scaling relations. *Macromolecules* **1994**, *27*, 3249−3261.

(12) Balastre, M.; Li, F.; Schorr, P.; Yang, J.; Mays, J. W.; Tirrell, M. V. A study of polyelectrolyte brushes formed from adsorption of amphiphilic diblock copolymers using the surface forces apparatus. *Macromolecules* **2002**, *35*, 9480−9486.

(13) Zhulina, E.; Borisov, O. Poisson−Boltzmann theory of pH-sensitive (annealing) polyelectrolyte brush. *Langmuir* **2011**, *27*, 10615−10633.

(14) Hollingsworth, N. R.; Wilkanowicz, S. I.; Larson, R. G. Salt-and pH-induced swelling of a poly (acrylic acid) brush via quartz crystal microbalance w/dissipation (QCM-D). *Soft Matter* **2019**, *15*, 7838−7851.

(15) Wu, T.; Gong, P.; Szleifer, I.; Vlček, P.; Šubr, V.; Genzer, J. Behavior of surface-anchored poly (acrylic acid) brushes with grafting density gradients on solid substrates: 1. Experiment. *Macromolecules* **2007**, *40*, 8756−8764.

(16) Chu, X.; Yang, J.; Liu, G.; Zhao, J. Swelling enhancement of polyelectrolyte brushes induced by external ions. *Soft Matter* **2014**, *10*, 5568−5578.
(17) Gong, P.; Wu, T.; Genzer, J.; Szleifer, I. Behavior of surface-anchored poly (acrylic acid) brushes with grafting density gradients on solid substrates: 2. Theory. *Macromolecules* **2007**, *40*, 8765−8773.
(18) Dong, R.; Lindau, M.; Ober, C. K. Dissociation behavior of weak polyelectrolyte brushes on a planar surface. *Langmuir* **2009**, *25*, 4774−4779.
(19) Ehtiati, K.; Moghaddam, S. Z.; Daugaard, A. E.; Thormann, E. How dissociation of carboxylic acid groups in a weak polyelectrolyte brush depend on their distance from the substrate. *Langmuir* **2020**, *36*, 2339−2348.
(20) Laloyaux, X.; Mathy, B.; Nysten, B.; Jonas, A. M. Bidimensional response maps of adaptive thermo-and pH-responsive polymer brushes. *Macromolecules* **2010**, *43*, 7744−7751.
(21) Lu, Y.; Zhuk, A.; Xu, L.; Liang, X.; Kharlampieva, E.; Sukhishvili, S. A. Tunable pH and temperature response of weak polyelectrolyte brushes: role of hydrogen bonding and monomer hydrophobicity. *Soft Matter* **2013**, *9*, 5464−5472.
(22) Johnson, E. C.; Willott, J. D.; Gresham, I. J.; Murdoch, T. J.; Humphreys, B. A.; Prescott, S. W.; Nelson, A.; de Vos, W. M.; Webber, G. B.; Wanless, E. J. Enrichment of charged monomers explains non-monotonic polymer volume fraction profiles of multi-stimulus responsive copolymer brushes. *Langmuir* **2020**, *36*, 12460−12472.
(23) Johnson, E. C.; Willott, J. D.; de Vos, W. M.; Wanless, E. J.; Webber, G. B. Interplay of composition, pH, and temperature on the conformation of multi-stimulus-responsive copolymer brushes: comparison of experiment and theory. *Langmuir* **2020**, *36*, 5765−5777.
(24) Johnson, E. C.; Gresham, I. J.; Prescott, S. W.; Nelson, A.; Wanless, E. J.; Webber, G. B. The direction of influence of specific ion effects on a pH and temperature responsive copolymer brush is dependent on polymer charge. *Polymer* **2021**, *214*, 123287.
(25) Yan, W.; Fantin, M.; Ramakrishna, S.; Spencer, N. D.; Matyjaszewski, K.; Benetti, E. M. Growing polymer brushes from a variety of substrates under ambient conditions by Cu0-mediated surface-initiated ATRP. *ACS Appl. Mater. Interfaces* **2019**, *11*, 27470−27477.
(26) Yan, W.; Fantin, M.; Spencer, N. D.; Matyjaszewski, K.; Benetti, E. M. Translating surface-initiated atom transfer radical polymerization into technology: The mechanism of Cu0-mediated si-atrp under environmental conditions. *ACS Macro Lett.* **2019**, *8*, 865−870.
(27) Zhang, T.; Du, Y.; Kalbacova, J.; Schubel, R.; Rodriguez, R. D.; Chen, T.; Zahn, D. R.; Jordan, R. Wafer-scale synthesis of defined polymer brushes under ambient conditions. *Polym. Chem.* **2015**, *6*, 8176−8183.
(28) Rauch, S.; Uhlmann, P.; Eichhorn, K.-J. In situ spectroscopic ellipsometry of pH-responsive polymer brushes on gold substrates. *Anal. Bioanal. Chem.* **2013**, *405*, 9061−9069.
(29) Willott, J. D.; Murdoch, T. J.; Humphreys, B. A.; Edmondson, S.; Webber, G. B.; Wanless, E. J. Critical salt effects in the swelling behavior of a weak polybasic brush. *Langmuir* **2014**, *30*, 1827−1836.
(30) Luxbacher, T. *The ZETA Guide: Principles of the Streaming Potential Technique*; Anton Paar GmbH: Graz, Austria, 2014.
(31) Chen, W.-L.; Cordero, R.; Tran, H.; Ober, C. K. 50th anniversary perspective: Polymer brushes: Novel surfaces for future materials. *Macromolecules* **2017**, *50*, 4089−4113.
(32) Zoppe, J. O.; Ataman, N. C.; Mocny, P.; Wang, J.; Moraes, J.; Klok, H.-A. Surface-initiated controlled radical polymerization: state-of-the-art, opportunities, and challenges in surface and interface engineering with polymer brushes. *Chem. Rev.* **2017**, *117*, 1105−1318.
(33) Grande, C. D.; Tria, M. C.; Jiang, G.; Ponnapati, R.; Advincula, R. Surface-grafted polymers from electropolymerized polythiophene RAFT agent. *Macromolecules* **2011**, *44*, 966−975.
(34) Barbey, R.; Laporte, V.; Alnabulsi, S.; Klok, H.-A. Postpolymerization modification of poly (glycidyl methacrylate) brushes: An XPS depth-profiling study. *Macromolecules* **2013**, *46*, 6151−6158.
(35) Ko, Y.; Genzer, J. Spontaneous degrafting of weak and strong polycationic brushes in aqueous buffer solutions. *Macromolecules* **2019**, *52*, 6192−6200.
(36) Uttley, O. F.; Brummitt, L. A.; Worrall, S. D.; Edmondson, S. Accessible and sustainable Cu (0)-mediated radical polymerisation for the functionalisation of surfaces. *Polym. Chem.* **2020**, *11*, 3831−3840.
(37) Che, Y.; Zhang, T.; Du, Y.; Amin, I.; Marschelke, C.; Jordan, R. On Water Surface-initiated Polymerization of Hydrophobic Monomers. *Angew. Chem., Int. Ed.* **2018**, *57*, 16380−16384.
(38) Alexander, S. Adsorption of chain molecules with a polar head a scaling description. *J. Phys.* **1977**, *38*, 983−987.
(39) de Gennes, P. Conformations of polymers attached to an interface. *Macromolecules* **1980**, *13*, 1069−1075.
(40) Varma, S.; Bureau, L.; Débarre, D. The conformation of thermoresponsive polymer brushes probed by optical reflectivity. *Langmuir* **2016**, *32*, 3152−3163.
(41) Yamamoto, S.; Ejaz, M.; Tsujii, Y.; Matsumoto, M.; Fukuda, T. Surface interaction forces of well-defined, high-density polymer brushes studied by atomic force microscopy. 1. Effect of chain length. *Macromolecules* **2000**, *33*, 5602−5607.
(42) Malham, I. B.; Bureau, L. Density effects on collapse, compression, and adhesion of thermoresponsive polymer brushes. *Langmuir* **2010**, *26*, 4762−4768.
(43) Borukhov, I.; Andelman, D.; Borrega, R.; Cloitre, M.; Leibler, L.; Orland, H. Polyelectrolyte titration: theory and experiment. *J. Phys. Chem. B* **2000**, *104*, 11027−11034.
(44) Petrov, A. I.; Antipov, A. A.; Sukhorukov, G. B. Base- acid equilibria in polyelectrolyte systems: From weak polyelectrolytes to interpolyelectrolyte complexes and multilayered polyelectrolyte shells. *Macromolecules* **2003**, *36*, 10079−10086.
(45) Lee, H.; Son, S. H.; Sharma, R.; Won, Y.-Y. A Discussion of the pH-Dependent Protonation Behaviors of Poly (2-(dimethylamino) ethyl methacrylate)(PDMAEMA) and Poly (ethylenimine-ran-2-ethyl-2-oxazoline)(P (EI-r-EOz)). *J. Phys. Chem. B* **2011**, *115*, 844−860.
(46) Cotanda, P.; Wright, D. B.; Tyler, M.; O'Reilly, R. K. A comparative study of the stimuli-responsive properties of DMAEA and DMAEMA containing polymers. *J. Polym. Sci., Part A: Polym. Chem.* **2013**, *51*, 3333−3338.
(47) Grace, J. L.; Huang, J. X.; Cheah, S.-E.; Truong, N. P.; Cooper, M. A.; Li, J.; Davis, T. P.; Quinn, J. F.; Velkov, T.; Whittaker, M. R. Antibacterial low molecular weight cationic polymers: Dissecting the contribution of hydrophobicity, chain length and charge to activity. *RSC Adv.* **2016**, *6*, 15469−15477.
(48) Willott, J. D.; Humphreys, B. A.; Murdoch, T. J.; Edmondson, S.; Webber, G. B.; Wanless, E. J. Hydrophobic effects within the dynamic pH-response of polybasic tertiary amine methacrylate brushes. *Phys. Chem. Chem. Phys.* **2015**, *17*, 3880−3890.
(49) Ferrand-Drake del Castillo, G.; Hailes, R. L.; Dahlin, A. Large changes in protonation of weak polyelectrolyte brushes with salt concentration-Implications for protein immobilization. *J. Phys. Chem. Lett.* **2020**, *11*, 5212−5218.
(50) Yadav, V.; Harkin, A. V.; Robertson, M. L.; Conrad, J. C. Hysteretic memory in pH-response of water contact angle on poly (acrylic acid) brushes. *Soft Matter* **2016**, *12*, 3589−3599.
(51) Ballauff, M.; Borisov, O. Polyelectrolyte brushes. *Curr. Opin. Colloid Interface Sci.* **2006**, *11*, 316−323.
(52) Lyatskaya, Y. V.; Leermakers, F.; Fleer, G.; Zhulina, E.; Birshtein, T. Analytical self-consistent-field model of weak polyacid brushes. *Macromolecules* **1995**, *28*, 3562−3569.
(53) Milner, S. T. Polymer brushes. *Science* **1991**, *251*, 905−914.
(54) Farzam, M.; Beitollahpoor, M.; Solomon, S. E.; Ashbaugh, H. S.; Pesika, N. S. Advances in the fabrication and characterization of superhydrophobic surfaces inspired by the Lotus leaf. *Biomimetics* **2022**, *7*, 196.
(55) Hunter, R. J. *Zeta Potential in Colloid Science: Principles and Applications*; Academic Press, 2013; Vol. 2.

https://doi.org/10.1021/acs.macromol.3c00947
Macromolecules 2023, 56, 9218−9228

(56) Bismarck, A.; Kumru, M. E.; Springer, J. Characterization of several polymer surfaces by streaming potential and wetting measurements: some reflections on acid−base interactions. *J. Colloid Interface Sci.* **1999**, *217*, 377−387.
(57) Jacobasch, H.-J. Characterization of solid surfaces by electrokinetic measurements. *Prog. Org. Coat.* **1989**, *17*, 115−133.
(58) Zimmermann, R.; Dukhin, S. S.; Werner, C.; Duval, J. F. On the use of electrokinetics for unraveling charging and structure of soft planar polymer films. *Curr. Opin. Colloid Interface Sci.* **2013**, *18*, 83−92.
(59) Childress, A. E.; Elimelech, M. Effect of solution chemistry on the surface charge of polymeric reverse osmosis and nanofiltration membranes. *J. Membr. Sci.* **1996**, *119*, 253−268.
(60) Bohinc, K.; Kralj-Iglič, V.; Iglič, A. Thickness of electrical double layer. Effect of ion size. *Electrochim. Acta* **2001**, *46*, 3033−3040.
(61) Guerrero-García, G. I.; González-Tovar, E.; Chávez-Páez, M.; Kłos, J.; Lamperski, S. Quantifying the thickness of the electrical double layer neutralizing a planar electrode: the capacitive compactness. *Phys. Chem. Chem. Phys.* **2018**, *20*, 262−275.
(62) Saboorian-Jooybari, H.; Chen, Z. Calculation of re-defined electrical double layer thickness in symmetrical electrolyte solutions. *Results Phys.* **2019**, *15*, 102501.
(63) Lai, P.-Y.; Lai, C.-Y. Polymer brush under strong shear. *Phys. Rev. E* **1996**, *54*, 6958−6961.
(64) Binder, K.; Kreer, T.; Milchev, A. Polymer brushes under flow and in other out-of-equilibrium conditions. *Soft Matter* **2011**, *7*, 7159−7172.
(65) Korolkovas, A.; Rodriguez-Emmenegger, C.; de los Santos Pereira, A.; Chenneviere, A.; Restagno, F.; Wolff, M.; Adlmann, F. A.; Dennison, A. J.; Gutfreund, P. Polymer brush collapse under shear flow. *Macromolecules* **2017**, *50*, 1215−1224.

https://doi.org/10.1021/acs.macromol.3c00947
Macromolecules 2023, 56, 9218−9228